AUTHOR(S):

Doi, Kazuki; Harper, Jonathan; Mollabashi, Ali; Takayanagi, Tadashi; Taki, Yusuke

京都大学学術情報リポジトリ

KURENAI 紅

Kyoto University Research Information Repository

京都大学
KYOTO UNIVERSITY

A Self-archived copy in
Kyoto University Research Information Repository
https://repository.kulib.kyoto-u.ac.jp

PHYSICAL REVIEW LETTERS **130,** 031601 (2023)

京都大学学術情報リポジトリ
KURENAI 紅
Kyoto University Research Information Repository

Pseudoentropy in dS/CFT and Timelike Entanglement Entropy

Kazuki Doi[ORCID],[1] Jonathan Harper[ORCID],[1] Ali Mollabashi[ORCID],[1] Tadashi Takayanagi[ORCID],[1,2,3] and Yusuke Taki[ORCID][1]

[1]*Center for Gravitational Physics, Yukawa Institute for Theoretical Physics, Kyoto University,*
Kitashirakawa Oiwakecho, Sakyo-ku, Kyoto 606-8502, Japan
[2]*Inamori Research Institute for Science, 620 Suiginya-cho, Shimogyo-ku, Kyoto 600-8411, Japan*
[3]*Kavli Institute for the Physics and Mathematics of the Universe, University of Tokyo, Kashiwa, Chiba 277-8582, Japan*

We study holographic entanglement entropy in dS/CFT and introduce timelike entanglement entropy in CFTs. Both of them take complex values in general and are related with each other via an analytical continuation. We argue that they are correctly understood as pseudoentropy. We find that the imaginary part of pseudoentropy implies an emergence of time in dS/CFT.

Introduction.—Holography in de Sitter (dS) space, so called the dS/CFT correspondence [1], has been much more mysterious than that in anti–de Sitter (AdS) space [2]. This is mainly because the dual conformal field theory (CFT) lives on a spacelike surface and the time coordinate emerges from a Euclidean CFT. Such CFTs turn out to be nonunitary, being exotic compared with text book examples of CFTs. Limited examples of CFTs dual to de Sitter spaces have been known in four dimensional higher spin gravity [3] and in three dimensional Einstein gravity [4,5]. Holography in two dimensional de Sitter space has also been developed [6,7]. The nonunitary nature of dual CFTs can be seen from the absence of spacelike geodesics between two distinct points on the dS boundary at future infinity. This makes the holographic entanglement entropy [8–10] complex valued [5,11–15].

In this Letter, we will argue this complex-valued quantity can be properly understood as pseudoentropy introduced in [16] (refer to [17] for a closely related quantity), rather than the standard entanglement entropy, which is real and non-negative. Pseudoentropy is defined as follows. Decomposing the total Hilbert space into those of subsystems A and B, we introduce the reduced transition matrix for two pure states $|\psi\rangle$ and $|\varphi\rangle$, by

$$\tau_A = \text{Tr}_B \left[\frac{|\psi\rangle\langle\varphi|}{\langle\varphi|\psi\rangle} \right]. \tag{1}$$

Finally, pseudoentropy is defined by

$$S_A = -\text{Tr}[\tau_A \log \tau_A]. \tag{2}$$

See Refs. [18–33] for further developments.

We consider pseudoentropy in dS/CFT because reduced density matrices in the dual Euclidean CFT are not Hermitian. Later, we will also point out that an imaginary part of entanglement entropy, which is properly understood as pseudoentropy, naturally arises in a timelike counterpart of entanglement entropy in standard CFTs. This is defined by rotating a spacelike subsystem into timelike one, via an analytical continuation. Indeed, we will show that the pseudoentropy in dS/CFT and the timelike entanglement entropy in AdS/CFT are directly related. Refer to [34–40] for earlier discussions on temporal extension of quantum entanglement, which are different from ours.

Pseudoentropy in dS/CFT.—Consider a $d+1$ dimensional de Sitter space (dS_{d+1}) in global coordinate,

$$ds^2 = R_{dS}^2(-d\tau^2 + \cosh^2\tau d\Omega_d^2). \tag{3}$$

We assume the Euclidean instanton, i.e., the semisphere

$$ds^2 = R_{dS}^2(d\tau_E^2 + \cos^2\tau_E d\Omega_d^2), \tag{4}$$

creates the de Sitter universe at $\tau_E = \tau = 0$ and later the Lorentzian evolution occurs following (3) for $\tau > 0$. Then in this setup of the dS/CFT [41], the gravity is dual to a Euclidean CFT on $\mathbb{S}^d$. We can define the reduced density matrix ρ_A by choosing a subsystem A on the equator of $\mathbb{S}^d$ as depicted in Fig. 1.

The dS/CFT relates the CFT partition function Z_{CFT} to the Hartle-Hawking wave function of dS [41]:

$$\Psi_{dS}[\phi_0] = Z_{\text{CFT}}[\phi_0], \tag{5}$$

where ϕ_0 is regarded in the bulk and boundary as a boundary condition for fields ϕ at the future boundary

京都大学
KYOTO UNIVERSITY

A Self-archived copy in
Kyoto University Research Information Repository
https://repository.kulib.kyoto-u.ac.jp

京都大学学術情報リポジトリ
KURENAI 紅
Kyoto University Research Information Repository
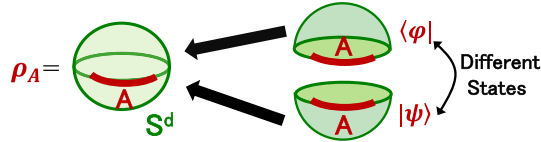
PHYSICAL REVIEW LETTERS 130, 031601 (2023)

FIG. 1. The reduced density matrix ρ_A of a CFT in dS/CFT gets non-Hermitian, which leads to pseudoentropy. Here, we consider a CFT on $\mathbb{S}^d$, i.e., the boundary of de Sitter space.

and a source in the dual CFT, respectively. The wave functional Ψ_{dS} is obtained by path integrating all fields:

$$\Psi_{dS}[\phi_0] = \int \mathcal{D}\phi \, e^{iS_G[\phi]} \Psi_0, \qquad (6)$$

where Ψ_0 denotes the initial state defined by a Euclidean path integral. Therefore, $Z_{CFT}[\phi_0]$ takes complex values in the classical saddle point approximation. Assuming $d = 2$ for simplicity, it is given by the Liouville action (this was evaluated in [42] for its complement region):

$$Z_{CFT} = e^{-S_E},$$
$$S_E = \frac{ic_{dS}}{24\pi} \int d^2x [(\partial_1\phi)^2 + (\partial_2\phi)^2 + \mu e^{2\phi}], \qquad (7)$$

where the metric on $\mathbb{S}^2$ is described by $ds^2 = e^{2\phi}(dx_1^2 + dx_2^2)$. Here, c_{dS} is defined by $c_{dS} = [(3R_{dS})/(2G_N)]$. Since the path integral on the north and south semisphere gives different states, the reduced density matrix ρ_A becomes non-Hermitian as illustrated in Fig. 1. In this way, the entanglement entropy in dS/CFT should more properly be regarded as the pseudoentropy. Similar treatment appears in the context of non-Hermitian condensed matter systems [43–45].

At $d = 2$, if we choose the subsystem A to be an arc with the angle θ_0 on the boundary $\mathbb{S}^2$, the geodesic distance L_A between the two boundaries of A leads to

$$S_A = \frac{L_A}{4G_N} = -i\frac{c_{dS}}{3} \log\left[\frac{2}{\epsilon}\sin\left(\frac{\theta_0}{2}\right)\right] + \frac{\pi c_{dS}}{6}, \qquad (8)$$

where the imaginary part comes from the timelike geodesic in (3) while the real part does from the spacelike one in (4), see Fig. 2. We introduced the UV cutoff ϵ of the CFT by $e^{\tau_\infty} = 2/\epsilon$. We can check that this geodesic indeed satisfies an extremization condition in a similar way to [5]. This condition requires that the spacelike geodesic should be the largest semicircle in the sphere. Thus, the real part does not depend on the size of A. Furthermore, this real part is identical to half the de Sitter entropy. Note that the de Sitter entropy is given by the length of largest circle in the full Euclidean dS$_3$. This is the holographic pseudoentropy in the global dS$_3$.
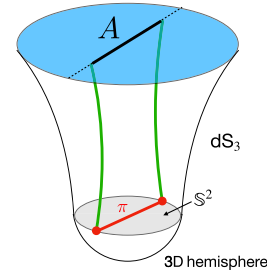

FIG. 2. The geodesic that reproduces the pseudoentropy (8).

In the Poincaré dS$_3$, $ds^2 = R_{dS}^2 \eta^{-2}(-d\eta^2 + dt_E^2 + dx^2)$, the holographic pseudoentropy for an interval A defined by $-x_0/2 \leq x \leq x_0/2$ at $t_E = 0$ reads

$$S_A = -i\frac{c_{dS}}{3} \log\left(\frac{x_0}{\epsilon}\right) + \frac{\pi c_{dS}}{6}. \qquad (9)$$

We can obtain these results (8) and (9) via the direct computation of geodesic lengths. It would be interesting to see if the path-integral optimization method [46,47] can derive these results for S_A in dS/CFT.

Timelike entanglement entropy as pseudoentropy.— Interestingly, when we extend entanglement entropy to timelike subsystems, which we call timelike entanglement entropy, we encounter complex values even for standard unitary CFTs. The entanglement entropy S_A for an interval A whose timelike and spacelike width are given by T_0 and X_0 reads

$$S_A = \frac{c_{AdS}}{3} \log\frac{\sqrt{X_0^2 - T_0^2}}{\epsilon}, \qquad (10)$$

where $c_{AdS} = [(3R_{AdS})/(2G_N)]$ is the central charge of the dual CFT [48,49]. The timelike entanglement entropy is obtained by setting $X_0 = 0$:

$$S_A = \frac{c_{AdS}}{3} \log\left(\frac{T_0}{\epsilon}\right) + \frac{i\pi c_{AdS}}{6}. \qquad (11)$$

We note that this is related to the pseudoentropy (9) in dS/CFT via an analytic continuation from AdS to dS: $R_{AdS} \to -iR_{dS}$, $z = -i\eta$, $t = -it_E$. We will argue that this quantity is also correctly regarded as pseudoentropy rather than entanglement entropy.

To see this, we consider its field theoretic calculation. For illustration purposes, consider a free scalar Φ with a mass m in two dimensions. The space and time coordinate are denoted by x and t, where the former is compactified with the periodicity β. The action of the scalar field reads

$$S_\Phi = \frac{1}{2}\int_{-\infty}^{\infty} dt \int_0^\beta dx[(\partial_t\Phi)^2 - (\partial_x\Phi)^2 - m^2\Phi^2]. \qquad (12)$$
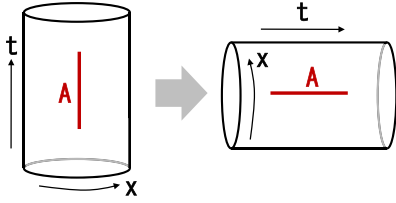
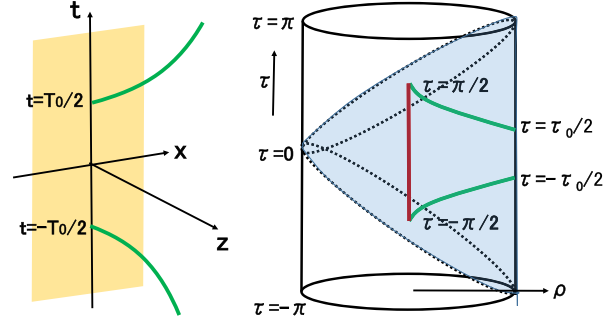FIG. 3.   Definition of timelike entanglement entropy.

FIG. 4.   The left panel shows the spacelike geodesic (green curve) in the Poincaré coordinate, which is embedded in the global coordinate with an additional timelike geodesic (red line) in the right panel.

Now, to calculate the timelike entanglement entropy, we regard t as the "space" direction and x as the Euclidean time by rotating the spacetime by ninety degree, depicted in Fig. 3. In this viewpoint we write the total partition function as

$$Z_\Phi = \text{Tr}[e^{-\beta \tilde{H}}], \tag{13}$$

where the "Hamiltonian" $\tilde{H}$ reads

$$\tilde{H} = -\frac{i}{2} \int_{-\infty}^{\infty} dt [\Pi^2 + (\partial_t \Phi)^2 - m^2 \Phi^2]. \tag{14}$$

Here, $\Pi = i\partial_x \Phi$ is the canonical momentum. In the massless case $m = 0$, in terms of the standard positive definite Hamiltonian (we again regard t as a space coordinate)

$$H_{\text{CFT}} = \frac{1}{2} \int_{-\infty}^{\infty} dt [\Pi^2 + (\partial_t \Phi)^2], \tag{15}$$

the partition function is rewritten as

$$Z_\Phi = \text{Tr}[e^{i\beta H_{\text{CFT}}}]. \tag{16}$$

If we trace out B, the reduced density matrix ρ_A reads

$$\rho_A = \text{Tr}_B[e^{i\beta H_{\text{CFT}}}], \tag{17}$$

which is not Hermitian. Note also that the timelike entanglement entropy is identical to the entanglement entropy at imaginary temperature.

We introduce two different states by doubling the Hilbert space similar to the thermofield double:

$$|\psi\rangle = \frac{1}{\sqrt{Z(\delta)}} \sum_n e^{i(\beta + i\delta)E_n/2} |n\rangle_1 |n\rangle_2,$$

$$|\varphi\rangle = \frac{1}{\sqrt{Z(\delta)}} \sum_n e^{-i(\beta - i\delta)E_n/2} |n\rangle_1 |n\rangle_2, \tag{18}$$

such that we obtain

$$\frac{\text{Tr}_2 |\psi\rangle\langle\varphi|}{\langle\varphi|\psi\rangle} = \frac{e^{i(\beta + i\delta)H}}{\text{Tr} e^{i(\beta + i\delta)H}}, \tag{19}$$

where δ is an infinitesimally small UV regulator. In this way, the timelike entanglement entropy for the reduced density matrix (17) is an example of pseudoentropy (2).

In the dual AdS$_3$, we can interpret the timelike entanglement entropy (11) as a geodesic length as follows. In the Poincaré coordinate, $ds^2 = R_{\text{AdS}}^2 z^{-2}(dz^2 - dt^2 + dx^2)$, the relevant geodesic is identified with $t = \sqrt{z^2 + T_0^2/4}$, via the Wick rotation of the familiar semicircle geodesic, depicted in the left panel of Fig. 4. Indeed its geodesic length

$$S_A = \frac{R_{\text{AdS}}}{4G_N} 2T_0 \int_\epsilon^\infty \frac{dz}{z\sqrt{z^2 + T_0^2/4}} = \frac{c}{3} \log \frac{T_0}{\epsilon} \tag{20}$$

explains the real part of (11). To understand the imaginary part, we embed Poincaré coordinate in global one: $ds^2 = R_{\text{AdS}}^2(-\cosh^2\rho \, d\tau^2 + d\rho^2 + \sinh^2\rho \, d\theta^2)$, as sketched in the right panel of Fig. 4. The Poincaré coordinate is covered by the blue region and therefore we need to connect the two end points at $\rho = 0$ and $\tau = \pm(\pi/2)$ by a timelike geodesic. Since the length is π, this explains the imaginal part $i\pi(c_{\text{AdS}}/6)$ of (11).

If we consider the timelike interval with the length τ_0 in the two dimensional CFT on a cylinder, the above global AdS$_3$ geodesic leads to the following estimation of the timelike entanglement entropy:

$$S_A = \frac{c_{\text{AdS}}}{3} \log \left[\frac{2}{\epsilon} \sin\left(\frac{\tau_0}{2}\right)\right] + \frac{c_{\text{AdS}}}{6} \pi i. \tag{21}$$

It is also useful to note that this can also be obtained by performing the analytical continuation $\beta \to -i\beta$ [remember (17)] on the known finite temperature CFT result for a length L interval A [49]

$$S_A = \frac{c_{\text{AdS}}}{3} \log \left[\frac{\beta}{\pi\epsilon} \sinh \frac{\pi L}{\beta}\right], \tag{22}$$

by setting $\beta = 2\pi$, $L = \tau_0$ with $\epsilon \to -i\epsilon$.

京都大学
KYOTO UNIVERSITY

A Self-archived copy in
Kyoto University Research Information Repository
https://repository.kulib.kyoto-u.ac.jp

PHYSICAL REVIEW LETTERS 130, 031601 (2023)

KURENAI 紅
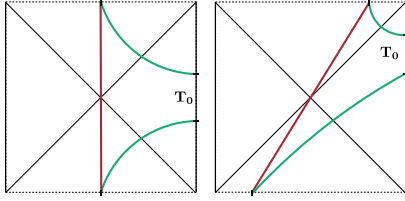Kyoto University Research Information Repository

FIG. 5. Space and timelike geodesics whose length gives the timelike holographic entanglement entropy in the BTZ geometry. For time intervals not symmetric about the origin (right panel) the spacelike geodesics intersect the past and future singularities in different locations.

At finite temperature, the gravity dual is given by the Bañados-Teitelboim-Zanelli (BTZ) black hole:

$$ds^2 = -(r^2 - r_+^2)dt^2 + \frac{dr^2}{r^2 - r_+^2} + r^2 d\phi^2, \quad (23)$$

where $r_+ = (2\pi/\beta)$. When A is a timelike interval with length T_0, the timelike entanglement entropy can be found again from the geodesic length, leading to

$$S_A = \frac{c_{\mathrm{AdS}}}{3} \log\left[\frac{\beta}{\pi\epsilon}\sinh\left(\frac{\pi}{\beta}T_0\right)\right] + \frac{c_{\mathrm{AdS}}}{6} i\pi. \quad (24)$$

The spacelike and timelike geodesic gives the real and imaginary part as depicted in Fig. 5.

Higher dimensional extension.—We can straightforwardly extend the above holographic calculations to higher dimensions. For simplicity, let us only consider the Poincaré AdS_{d+1}

$$ds^2 = R_{\mathrm{AdS}}^2 \frac{dz^2 - dt^2 + dy^2 + d\mathbf{x}^2}{z^2}, \quad (25)$$

where y is a direction that we regard as an alternative "time" and $\mathbf{x} \in \mathbb{R}^{d-2}$ are the remaining directions. Here, we take a hyperbolic subsystem A defined by $t^2 - \mathbf{x}^2 \geq T_0^2/4$ as a generalization of a temporal interval in the $d = 2$ case. Introducing a radial coordinate $\xi = \sqrt{t^2 - \mathbf{x}^2}$ for the unit $\mathbb{H}^{d-2}$, the holographic entanglement entropy is evaluated by varying a functional

$$S_A = \frac{R_{\mathrm{AdS}}^{d-1}}{4G_N^{(d+1)}} \mathrm{Vol}(\mathbb{H}^{d-2}) \int dz \frac{\xi^{d-2}}{z^{d-1}} \sqrt{1 - \xi'(z)^2}, \quad (26)$$

with a boundary condition $\xi(0) = T_0/2$. The resulting extremal surface is the union of a spacelike surface $\xi^2 - z^2 = (T_0^2/4)$ and a timelike surface $z^2 - \xi^2 = (T_0^2/4)$. This can be regarded as a generalization of Fig. 4 in $d = 2$. Thus, we find

$$S_A = \frac{R_{\mathrm{AdS}}^{d-1}}{4G_N^{(d+1)}} \mathrm{Vol}(\mathbb{H}^{d-2}) \left[\sum_{k=0}^{\frac{d-3}{2}} \frac{\binom{\frac{d-3}{2}}{k}}{d-2k-2} \left(\frac{T_0}{2\epsilon}\right)^{d-2k-2} + \frac{i\sqrt{\pi}\Gamma(\frac{d-1}{2})}{2\Gamma(\frac{d}{2})}\right], \quad (27)$$

for odd d and

$$S_A = \frac{R_{\mathrm{AdS}}^{d-1}}{4G_N^{(d+1)}} \mathrm{Vol}(\mathbb{H}^{d-2}) \left[\sum_{k=0}^{\frac{d}{2}-2} \frac{\binom{\frac{d-3}{2}}{k}}{d-2k-2} \left(\frac{T_0}{2\epsilon}\right)^{d-2k-2} + \frac{\Gamma(\frac{d-1}{2})}{\sqrt{\pi}\Gamma(\frac{d}{2})}\log\left(\frac{T_0}{2\epsilon}\right) + \frac{i\sqrt{\pi}\Gamma(\frac{d-1}{2})}{2\Gamma(\frac{d}{2})}\right], \quad (28)$$

for even d, where $\mathrm{Vol}(\mathbb{H}^{d-2})$ denotes the volume of $\mathbb{H}^{d-2}$, assumed to be properly regularized.

We can relate this result (27) to the entanglement entropy for a spherical region [9] in Euclidean AdS_{d+1} by an analytic continuation $T_0 \rightarrow -iT_0$, $\mathrm{Vol}(\mathbb{H}^{d-2}) \rightarrow i^{d-2}\mathrm{Vol}(\mathbb{S}^{d-2})$. After that, by taking another analytic continuation from EAdS to dS; $R_{\mathrm{AdS}} \rightarrow -iR_{\mathrm{dS}}$, $\epsilon \rightarrow -i\epsilon$, we obtain the pseudoentropy for $\mathrm{dS}_{d+1}/\mathrm{CFT}_d$. It is remarkable that the resulting pseudoentropy has the real part

$$\frac{R_{\mathrm{dS}}^{d-1}\pi^{d/2}}{4G_N^{(d+1)}\Gamma(\frac{d}{2})}, \quad (29)$$

which is identical to a half of the de Sitter entropy in dS_{d+1}. When $d = 2$, this reduces to the real part $\pi c_{\mathrm{dS}}/6$ of (8). On the other hand, all the divergent terms are purely imaginary, which come from the timelike extremal surfaces in (3).

Numerical analysis.—Here, we present our numerical checks for the timelike entanglement entropy illustrated in Fig. 3 for 2D free scalar and free Dirac fermion theories. We adapt the correlator method [50–52] to analyze timelike entanglement. For the case of a continuous spatial direction and discrete time direction on an infinite lattice, the relevant correlators for a pure timelike region in the scalar theory are given by

$$\mathrm{Tr}[e^{-\beta\tilde{H}}\Phi(t)\Phi(t')] = \int_{-\pi}^{\pi} \frac{dk}{2\pi} \coth\frac{-i\beta\omega_\Phi}{2} \frac{1}{2\omega_\Phi} e^{ik(t-t')},$$

$$\mathrm{Tr}[e^{-\beta\tilde{H}}\Pi(t)\Pi(t')] = \int_{-\pi}^{\pi} \frac{dk}{2\pi} \frac{\omega_\Phi \coth\frac{-i\beta\omega_\Phi}{2}}{2} e^{ik(t-t')}, \quad (30)$$

where $\omega_\Phi(k) = \sqrt{m^2 + (4/\epsilon^2)\sin^2(k/2)}$ and for the Dirac fermion theory the correlators are given by

$$\mathrm{Tr}[e^{-\beta\tilde{H}}\Psi^\dagger(t)\Psi(t')] = \frac{\delta_{t,t'}}{2}\mathbf{1} - \int_{-\pi}^{\pi} \frac{dk}{2\pi} \frac{\tanh(-i\beta\omega_\Psi)}{2\omega_\Psi}$$

$$\times \begin{pmatrix} \sin k & m \\ m & -\sin k \end{pmatrix} e^{ik(t-t')}, \quad (31)$$

京都大学
KYOTO UNIVERSITY

A Self-archived copy in
Kyoto University Research Information Repository
https://repository.kulib.kyoto-u.ac.jp

PHYSICAL REVIEW LETTERS 130, 031601 (2023)

京都大学学術情報リポジトリ
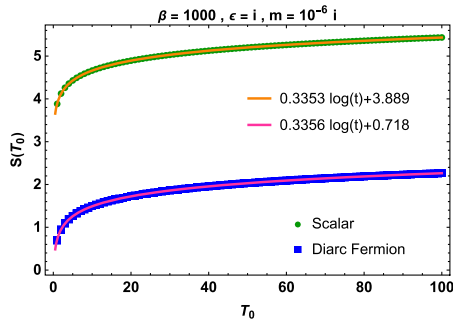KURENAI 紅
Kyoto University Research Information Repository

FIG. 6. Numerical results for timelike entanglement and the corresponding fit functions for free scalar and Dirac theories.

where $\omega_\Psi(k) = \sqrt{m^2 + (1/\epsilon^2)\sin^2 k}$ (for our conventions see the appendix of [53]). The important point in both theories is that these correlation functions are the same as the thermal state correlators in a theory with a standard Hamiltonian after applying the analytic continuation $\beta \to -i\beta$. The nontrivial point for our definition of timelike Hamiltonian is that as the expression of $\tilde{H}$ and Fig. 3 are hinting, we apply $m \to im$ (the IR regulator in the CFT case) and $\epsilon \to -i\epsilon$ (the UV cutoff) in these correlators in order to get timelike entanglement entropy. Figure 6 shows our numerical results which perfectly agree with our analytic results.

It is worthwhile to note that the imaginary part can be also captured in our numerical method by considering more general regularization prescriptions such as $\epsilon \to -i^a\epsilon$, where a is a real number. The value of a solely affects the coefficient of the imaginary part, which is independent of the subregion length.

Discussions.—In this Letter, we argued holographic entanglement entropy in dS/CFT and timelike entanglement entropy in ordinary CFTs both should correctly be understood as pseudoentropy. They are related to each other via an analytical continuation. Our results strongly imply the imaginary part of pseudoentropy describes an emergence of time coordinate in holography. This generalizes an emergent space from quantum entanglement [54,55]. We expect this will help us understand the basic mechanism of emergent time in dS/CFT in the near future.

Note added.—Recently, we noted the preprint [56], which also analyzes timelike entanglement entropy, and the preprint [57], which has a partial overlap.

[1] A. Strominger, J. High Energy Phys. 10 (2001) 034.
[2] J. M. Maldacena, Adv. Theor. Math. Phys. 2, 231 (1998).
[3] D. Anninos, T. Hartman, and A. Strominger, Classical Quantum Gravity 34, 015009 (2017).
[4] Y. Hikida, T. Nishioka, T. Takayanagi, and Y. Taki, Phys. Rev. Lett. 129, 041601 (2022).
[5] Y. Hikida, T. Nishioka, T. Takayanagi, and Y. Taki, J. High Energy Phys. 05 (2022) 129.
[6] J. Maldacena, G. J. Turiaci, and Z. Yang, J. High Energy Phys. 01 (2021) 139.
[7] J. Cotler, K. Jensen, and A. Maloney, J. High Energy Phys. 06 (2020) 048.
[8] S. Ryu and T. Takayanagi, Phys. Rev. Lett. 96, 181602 (2006).
[9] S. Ryu and T. Takayanagi, J. High Energy Phys. 08 (2006) 045.
[10] V. E. Hubeny, M. Rangamani, and T. Takayanagi, J. High Energy Phys. 07 (2007) 062.
[11] K. Narayan, Phys. Rev. D 91, 126011 (2015).
[12] Y. Sato, Phys. Rev. D 91, 086009 (2015).
[13] M. Miyaji and T. Takayanagi, Prog. Theor. Exp. Phys. 2015, 073B03 (2015).
[14] K. Narayan, Phys. Lett. B 779, 214 (2018).
[15] K. Narayan, Phys. Rev. D 101, 086014 (2020).
[16] Y. Nakata, T. Takayanagi, Y. Taki, K. Tamaoka, and Z. Wei, Phys. Rev. D 103, 026005 (2021).
[17] S. Murciano, P. Calabrese, and R. M. Konik, J. High Energy Phys. 05 (2022) 152.
[18] A. Mollabashi, N. Shiba, T. Takayanagi, K. Tamaoka, and Z. Wei, Phys. Rev. Lett. 126, 081601 (2021).
[19] G. Camilo and A. Prudenziati, arXiv:2101.02093.
[20] A. Mollabashi, N. Shiba, T. Takayanagi, K. Tamaoka, and Z. Wei, Phys. Rev. Res. 3, 033254 (2021).
[21] T. Nishioka, T. Takayanagi, and Y. Taki, J. High Energy Phys. 09 (2021) 015.
[22] K. Goto, M. Nozaki, and K. Tamaoka, Phys. Rev. D 104, L121902 (2021).
[23] M. Miyaji, J. High Energy Phys. 12 (2021) 013.
[24] I. Akal, T. Kawamoto, S.-M. Ruan, T. Takayanagi, and Z. Wei, Phys. Rev. D 105, 126026 (2022).
[25] M. Berkooz, N. Brukner, S. F. Ross, and M. Watanabe, J. High Energy Phys. 08 (2022) 051.
[26] I. Akal, T. Kawamoto, S.-M. Ruan, T. Takayanagi, and Z. Wei, J. High Energy Phys. 08 (2022) 296.
[27] T. Mori, H. Manabe, and H. Matsueda, Phys. Rev. D 106, 086008 (2022).
[28] J. Mukherjee, J. High Energy Phys. 10 (2022) 016.
[29] W.-z. Guo, S. He, and Y.-X. Zhang, J. High Energy Phys. 09 (2022) 094.
[30] Y. Ishiyama, R. Kojima, S. Matsui, and K. Tamaoka, Prog. Theor. Exp. Phys. 2022, 093B10 (2022).
[31] M. Miyaji and C. Murdia, J. High Energy Phys. 11 (2022) 123.
[32] A. Bhattacharya, A. Bhattacharyya, and S. Maulik, Phys. Rev. D 106, 086010 (2022).

[33] W.-z. Guo, S. He, and Y.-X. Zhang, arXiv:2209.07308.

[34] A. J. Leggett and A. Garg, Phys. Rev. Lett. **54**, 857 (1985).

[35] J. Fitzsimons, J. Jones, and V. Vedral, arXiv:1302.2731.

[36] S. J. Olson and T. C. Ralph, Phys. Rev. A **85**, 012306 (2012).

[37] J. Cotler, C.-M. Jian, X.-L. Qi, and F. Wilczek, J. High Energy Phys. 09 (2018) 093.

[38] J. Cotler *et al.*, Phys. Rev. X **9**, 031013 (2019).

[39] A. Lerose, M. Sonner, and D. A. Abanin, Phys. Rev. B **104**, 035137 (2021).

[40] G. Giudice, G. Giudici, M. Sonner, J. Thoenniss, A. Lerose, D. A. Abanin, and L. Piroli, Phys. Rev. Lett. **128**, 220401 (2022).

[41] J. M. Maldacena, J. High Energy Phys. 05 (2003) 013.

[42] J. Boruch, P. Caputa, D. Ge, and T. Takayanagi, J. High Energy Phys. 07 (2021) 016.

[43] R. Couvreur, J. L. Jacobsen, and H. Saleur, Phys. Rev. Lett. **119**, 040601 (2017).

[44] L. Herviou, N. Regnault, and J. H. Bardarson, SciPost Phys. **7**, 069 (2019).

[45] P.-Y. Chang, J.-S. You, X. Wen, and S. Ryu, Phys. Rev. Res. **2**, 033069 (2020).

[46] P. Caputa, N. Kundu, M. Miyaji, T. Takayanagi, and K. Watanabe, Phys. Rev. Lett. **119**, 071602 (2017).

[47] P. Caputa, N. Kundu, M. Miyaji, T. Takayanagi, and K. Watanabe, J. High Energy Phys. 11 (2017) 097.

[48] C. Holzhey, F. Larsen, and F. Wilczek, Nucl. Phys. **B424**, 443 (1994).

[49] P. Calabrese and J. L. Cardy, J. Stat. Mech. (2004) P06002.

[50] I. Peschel, J. Phys. A **36**, L205 (2003).

[51] J. I. Latorre, E. Rico, and G. Vidal, Quantum Inf. Comput. **4**, 48 (2004).

[52] H. Casini and M. Huerta, J. Phys. A **42**, 504007 (2009).

[53] M. R. M. Mozaffar and A. Mollabashi, Phys. Rev. Res. **4**, L022010 (2022).

[54] M. Van Raamsdonk, Gen. Relativ. Gravit. **42**, 2323 (2010).

[55] B. Swingle, Phys. Rev. D **86**, 065007 (2012).

[56] B. Liu, H. Chen, and B. Lian, arXiv:2210.03134.

[57] K. Narayan, arXiv:2210.12963.